Roles of Disulfide Bonds in Recombinant Human Interleukin 6 Conformation†

Fernando L. Rock,‡ Xiaomao Li,§ Pele Chong,‖ Nobou Ida,⊥ and Michel Klein*,‡,§,‖

Departments of Biochemistry and Immunology, University of Toronto, Toronto, Ontario M5S 1A8, Canada, The Connaught Centre for Biotechnology Research, Willowdale, Ontario M2R 3T4, Canada, and Basic Research Laboratories, Toray Industries Inc., 1111 Tebiro Kamakura, Kanagawa, 248 Japan

Received June 22, 1993; Revised Manuscript Received September 22, 1993®

ABSTRACT: Human IL-6 has two disulfide bonds linking Cys_{45} to Cys_{51} and Cys_{74} to Cys_{84}, respectively. Previous site-directed mutagenesis studies have demonstrated that the Cys_{74}–Cys_{84} bond is essential for full biological and receptor binding activities. To address the structural importance of these disulfide bonds in the formation and stabilization of IL-6 secondary and tertiary structures, we have generated a panel of disulfide bond-deficient rIL-6 analogs both by chemical reduction and alkylation as well as by site-directed mutagenesis. Conformational changes affecting these rIL-6 analogs were probed by circular dichroism spectroscopy, as well as reactivity with monoclonal antibodies, and correlated with changes in biological activities. We have shown that the first disulfide bridge (Cys_{45}–Cys_{51}) is highly sensitive to reduction and, therefore, more solvent-exposed or less thermodynamically stable. Contrary to previous reports, this bridge contributes, although minimally, to the full biological activity of the cytokine. However, no significant changes in secondary or tertiary structures were observed upon removal of this bond. In marked contrast, analogs lacking the disulfide bridge between Cys_{74} and Cys_{84} exhibited as little as 0.5% and 0.05% wild-type biological and receptor binding activities, respectively. These dramatic changes correlated with a slight reduction in α-helical content and a decreased reactivity with the neutralizing monoclonal antibody mAb8 which recognizes a conformational epitope associated with the active site. Our results suggest that the second disulfide bridge plays a critical role in maintaining the spatial relationship between the putative IL–6 A and D helices.

Interleukin 6 (IL-6)[1] is a 26-kDa glycoprotein produced by a variety of cell types and is involved in numerous biological functions including B-cell and neural cell differentiation, T-cell maturation, hematopoiesis, and the induction of acute-phase proteins [reviewed in Van Snick (1990)]. In addition, dysregulated IL-6 overexpression *in vivo* has been associated with the pathogenesis of several human diseases such as myelomas and plasmacytomas, AIDS, alcohol liver cirrhosis, glomerulonephritis, psoriasis, and rheumatoid arthritis [reviewed in Hirano et al. (1990)]. Nevertheless, clinical trials have demonstrated potential beneficial effects of rIL-6 in the treatment of myeloid leukemia, breast cancer, and bone marrow transplants [reviewed in Hirano et al. (1990)].

Efforts to design therapeutic agents based on rIL-6 analogs are currently limited by the lack of IL-6 crystallographic or NMR structural information. Nonetheless, cloning of the IL-6 cDNA has indicated that the molecule consists of 185 amino acids (21 kDa) including 4 cysteine residues and 2 potential sites for N-linked glycosylation (Hirano et al., 1986). However, glycosylation is not necessary for biological activity (Rock et al., 1992). Circular dichroism studies have revealed that the cytokine has essentially an α-helical structure (70%) in solution (Krüttgen et al., 1990; Rock et al., 1992). Comparative modeling analysis of IL-6 and other growth factors related by evolution including the human growth hormone (hGRH) (DeVos et al., 1992) and the human granulocyte colony stimulating factor (G-CSF) (Hill et al., 1993), for which crystal structures have been determined, suggests that IL-6 folds as a four α-helix bundle protein (Bazan, 1990). X-ray diffraction analyses of hGRH and hG-CSF has revealed that these molecules consist of two long and two short closely packed, antiparallel α-helices (labeled A–D) connected by one short and two long, criss-crossing peptide loops with some defined secondary structures. Deletion map analyses and site-directed mutagenesis studies have demonstrated that, like hGRH (DeVos et al., 1992), the primary receptor binding site of IL-6 involves residues from both the N- and C-terminal ends of the molecule (Brakenhoff et al., 1989; Krüttgen et al., 1990; Fiorillo et al., 1992). Although some neutralizing monoclonal antibodies, such as mAb8 (Brakenhoff et al., 1990), specifically recognize a major conformational epitope associated with this site, the possibility of secondary binding sites recognized by other neutralizing monoclonal antibodies, such as IG61 (Ida et al., 1989), should not be excluded.

The four IL-6 cysteine residues form two intrachain disulfide bonds between Cys_{45} and Cys_{51} and between Cys_{74} and Cys_{84}, respectively (Clogston et al., 1989). Interestingly, the number, location, and disulfide linkage pattern of these cysteines are

† This work was supported by Grants MT-4259 and MT-6780 (M.K.) of the Medical Research Council of Canada.

* Author to whom correspondence should be addressed at the Department of Immunology, Medical Sciences Building, University of Toronto, Ontario M5S 1A8, Canada. Telephone: 978-6258. FAX: 416-978-1938.

‡ Department of Biochemistry, University of Toronto.

§ Department of Immunology, University of Toronto.

‖ The Connaught Centre for Biotechnology Research.

⊥ Toray Industries Inc.

® Abstract published in *Advance ACS Abstracts,* April 1, 1994.

[1] Abbreviations: r, recombinant; IL, interleukin; HPLC, high-performance liquid chromatography; DTT, dithiothreitol; SDS–PAGE, sodium dodecyl sulfate–polyacrylamide gel electrophoresis; TFA, trifluoroacetic acid; CD, circular dichroism; GuHCl, guanidine hydrochloride; BSA, bovine serum albumin; FCS, fetal calf serum; PBS, phosphate-buffered saline; EBV, Epstein Barr virus; mAb, monoclonal antibody; TCA, trichloroacetic acid; ELISA, enzyme-linked immunosorbent assay; Ig, immunoglobulin; hGRH, human growth hormone; hG-CSF, human granulocyte colony stimulating factor; Wt, wild-type; 1-reduced, one-bridge reduced and alkylated rIL-6; 2-reduced, two-bridge reduced and alkylated rIL-6; PTH, phenylthiohydantoin.

0006-2960/94/0433-5146$04.50/0

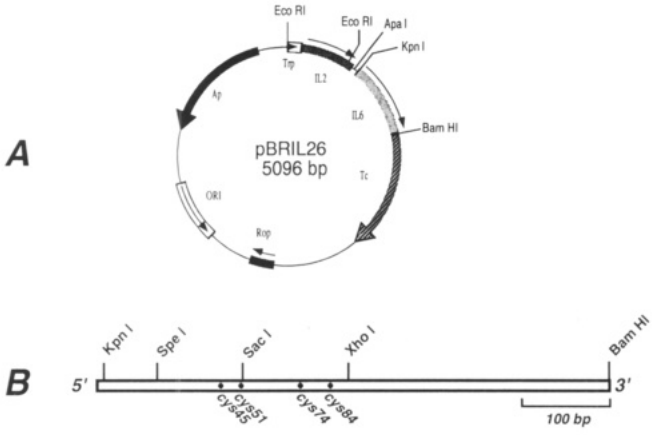

FIGURE 1: High-level rIL-6 expression vector. Schematic representation of the expression vector pBRIL26 (A) used for the construction and overexpression of wild-type IL-6 and alanine analog genes. Trp, tryptophan promoter; IL2, IL-2 cDNA sequence; IL6, IL-6 cDNA sequence. All rIL-6 molecules were expressed as rIL-2/IL-6 fusion proteins under the control of the *trp* promoter. (B) Partial restriction map of the IL-6 cDNA indicating positions of the *Spe*I/*Sac*I and *Sac*I/*Xho*I synthetic oligonucleotides cassettes used for Cys to Ala mutagenesis. Dots indicate the positions of nucleotide triplets coding for cysteine residues.

highly conserved among murine IL-6 (Simpson et al., 1988; Tanabe et al., 1988), human IL-6 (Clogston et al., 1989), murine G-CSF (Tsuchiya et al., 1986), human G-CSF (Lu et al., 1989), and chicken myelomonocytic growth factor (cMGF) (Leutz et al., 1989), suggesting that these cysteines and disulfide bonds play important structural and/or functional roles. Hence, IL-6 cysteines have been the targets for structure–function studies (Jambou et al., 1988; Snouwaert et al., 1991a,b; Jean et al., 1993). Results from mutagenesis experiments have revealed that only the second disulfide bridge (Cys_{74}–Cys_{84}) is essential for IL-6 bioactivity and receptor binding. However, to date, there is no experimental evidence to explain how the lack of the second disulfide bridge affects the structure of the receptor binding site(s). To specifically address this question, we have generated both chemical and genetic rIL-6 cysteine analogs to determine the respective role of the two disulfide bridges in IL-6 folding and in the stabilization of its α-helical secondary structure as well as their respective contribution to the tertiary conformation of the receptor binding site(s). We have demonstrated that the two disulfide bonds are differentially sensitive to reduction, that the first bridge participates, although minimally, to the biological activity of the cytokine, and that the second bond is critical to the formation and stabilization of the spatial relationship between the putative A and D helix segments forming the primary IL-6 receptor binding site.

MATERIALS AND METHODS

Expression and Purification of Native rIL-6 and rIL-6 Analogs. Expression and purification of native human rIL-6 and analogs were performed as previously described by Rock et al. (1992). Briefly, the high-level expression vector pBRIL26 (Figure 1A) was used to produce wild-type rIL-6 and rIL-6 variants linked to the C-terminus of IL-2 by a collagen-like spacer. The rIL-6 coding region of this expression vector was synthesized to contain several unique restriction sites, without altering the IL-6 primary amino acid sequence, to facilitate genetic manipulations (Figure 1B). Thus, rIL-6 analogs in which pairs of cysteines were replaced by alanine residues were constructed by cassette insertion mutagenesis. Complementary oligonucleotides were synthesized on an Applied Biosystems Model 380A DNA synthesizer. A 99-mer *Spe*I–*Sac*I cassette was used to generate the $Ala_{45}/Alal_{51}$ mutant (rIL-6 $Ala_{45,51}$), while a 125-mer *Sac*I–*Xho*I cassette was used to engineer the Ala_{74}/Ala_{84} variant (rIL-6 $Ala_{74,84}$). The rIL-6 $Ala_{45,51,74,84}$ analog was constructed using both the 99-mer and 125-mer cassettes. Restriction endonucleases were purchased from Boehringer Mannheim and Pharmacia Biochemicals. All cloning methods were performed as described by Sambrook et al. (1989), and mutations were confirmed by dideoxy sequence determination.

Constructs were transformed into *Escherichia coli* (strain HB101), and rIL-6 analogs were overexpressed as insoluble IL-2/IL-6 fusion proteins after induction of the pBRIL26 *Trp* promoter with 3-β-indoleacrylic acid. Bacterial cells were lysed in a French pressure cell (20 000 lb/in.^{2}) and inclusion bodies isolated by 10-min centrifugation at 5000*g*. Fusion proteins were dissolved in 6 M guanidine hydrochloride and then refolded and reoxidized by dilution in a redox buffer (0.1 M Tris-HCl, pH 8.6) containing 10 mM reduced and 1 mM oxidized glutathione. Recombinant IL-6 analogs were separated from rIL-2 by collagenase digestion, then purified to homogeneity by reverse-phase HPLC, lyophilized, and stored as powders at −20 °C until required as previously described (Rock et al., 1992).

Reduction and Alkylation of Native rIL-6. All reduction experiments were carried out with 50- or 100-μL aliquots of rIL-6 at a concentration of 10 μM in 0.1 M Tris-HCl, pH 8.6. To determine the relative sensitivity of the rIL-6 disulfide bonds to reducing agents, reduction experiments were carried out in the presence of increasing DTT concentrations (0–10 mM) for 1 h at 37 °C. Proteins were then alkylated with 25 mM iodoacetic acid for 30 min at room temperature. Experiments to evaluate the time required for full rIL-6 reduction were performed as follows. Reduction was first initiated by the addition of 5 mM DTT at 37 °C. Aliquots from the reaction were then removed at regular intervals between 0 and 45 min, at which time reduction was stopped by alkylation with iodoacetic acid. Analysis of the effect of temperature on reduction was determined by reducing rIL-6 at increasing temperatures (25, 28, 31, 34, and 37 °C) for 1 h in the presence of 5 mM DTT followed by alkylation. Products from these various reduction/alkylation experiments were then subjected to SDS–PAGE (15 or 20%) for mobility shift analysis.

To assess the effect of the alkylating agent on biological activity, rIL-6 (10 μM) was reduced with either 50 μM or 5 mM DTT for 1 h at 37 °C and then alkylated for 15 min at room temperature with 25 mM either iodoacetic acid, iodoacetamide, or methyl iodide. After confirmation of reduction by SDS–PAGE analysis, samples were exhaustively dialyzed against phosphate-buffered saline, pH 7.4 (PBS) at 4 °C.

Identification of the IL-6 Labile Disulfide Bridge. Two hundred micrograms of wild-type rIL-6 in 1 mL of 0.1 M Tris-HCl, pH 8.6, was reduced with 50 μM DTT for 1 h at 37 °C. The sample was then alkylated with 200 μM [2-^{3}H]-iodoacetic acid (specific activity 185 GBq/mmol, Amersham) for 30 min at room temperature. Radiolabeled rIL-6 was precipitated with 10% trichloroacetic acid (TCA), washed twice with 4% TCA, and redissolved in 200 μL of 0.2 M ammonium bicarbonate, pH 7.8. IL-6 was then digested with *Staphylococcus aureus* V8 protease (type XVII-B, Sigma) at an enzyme to substrate ratio of 1:50 (w/w) for 24 h at 37 °C. IL-6 peptides were subsequently separated by reverse-phase HPLC using an analytical Vydac C_{18} column (218TP104;

Scientific Products & Equipment Limited, Ontario, Canada) operated at a flow rate of 0.8 mL/min. Chromatography was carried out using a TFA/acetonitrile gradient system in which the mobile phase A was 0.1% TFA and B was 0.1% TFA in 90% acetonitrile, respectively. Peptide elution was monitored by UV absorbance at 215 nm and radioactivity measured using a Searle Analytic Model 6892 liquid scintillation counter. Peptides were first separated with a linear gradient from 100% A/0% B to 40% A/60% B over 60 min followed by a 10-min 10% A/90% B wash. Fractions were collected at 2-min intervals; radioactive samples were pooled, lyophilized, and rechromatographed using a linear gradient from 100% A/0% B to 80% A/20% B over 60 min followed by a 10-min 10% A/90% B wash. Peaks were collected manually, and the radioactive fractions were lyophilized and subjected to microsequence analysis for identification.

Microsequencing. N-Terminal microsequence analysis of the IL-6 peptide fragment was performed by automated Edman degradation using an Applied Biosystems Model 4778 sequenator. Protocols were performed according to the manufacturer's instructions. Radiolabeled *S*-carboxymethylated cysteine residues were identified by HPLC analysis using an ABI Microbore Model 120A amino acid analyzer and *S*-(carboxymethyl)cysteine PTH-derivatives as standards, as well as by scintillation counting following each cycle of Edman degradation.

SDS–PAGE Analysis. Wild-type rIL-6 and rIL-6 analogs were analyzed by SDS–PAGE in either 15% or 20% acrylamide gels under both nonreducing and reducing conditions, as described by Laemmli et al. (1970). Gels were stained with 0.1% Coomassie blue in 50% methanol and 10% acetic acid followed by diffusion destaining in a solution of 5% methanol and 10% acetic acid. Molecular mass markers (14.4–94 kDa) were obtained from Pharmacia.

Determination of Protein Concentration. Concentrations of rIL-6 and rIL-6 analogs were determined spectrophotometrically at 280 nm using an extinction coefficient ($E^{1\%}_{1cm}$) of 4.6 (Rock et al., 1992).

Circular Dichroism (CD) Measurements. Wild-type rIL-6 and alanine analogs were dissolved in water for CD analyses. Native, partially (1-bridge) and fully reduced/alkylated rIL-6 species were extensively dialyzed against and diluted in 150 mM NaCl/1 mM Tris-HCl, pH 7.4. Far-UV CD spectra (200–260 nm) were performed at room temperature in a 0.1-cm quartz cuvette using a Jasco Model J-41A spectropolarimeter calibrated with an aqueous solution of *d*-camphorsulfonic acid. After substraction of solvent spectra, data were expressed as mean residue ellipticities (MRE) calculated using 114 as the mean residue weight of rIL-6. The method of Provencher and Glöckner (1981) was used to convert ellipticity data into conformational parameters.

Denaturation Experiments. Stock solutions of optical-grade guanidine hydrochloride (RNase grade, Sigma) in 0.1 M Tris-HCl, pH 8.6, were prepared in concentrations ranging from 0 to 6 M. Stock solutions of wild-type rIL-6 (2.0 mg/mL) and the rIL-6 $Ala_{45,51,74,84}$ mutant (1.5 mg/mL) were diluted 20-fold in 0.5 mL each of guanidine hydrochloride and of stock solution and then equilibrated for 4 h at room temperature before CD analysis. Ellipticities were measured at 220 nm in a 0.1-cm cuvette at room temperature. After subtraction of the respective solvent backgrounds, data were expressed as percentages relative to the ellipticity obtained in the absence of guanidine, chosen as 100%. Denaturation of fully reduced, but not alkylated, rIL-6 was performed as described above except that rIL-6 was first reduced with 10 mM DTT/0.1 M Tris-HCl, pH 8.6, for 1 h at 37 °C and then diluted in varying concentrations of guanidine hydrochloride in 0.1 M Tris-HCl, pH 8.6, in the presence of 2 mM DTT to prevent reoxidation. Full reduction was confirmed by SDS–PAGE mobility shift analysis.

The free energy of α-helix denaturation in the absence of denaturant ($\Delta G_D^{H_2O}$) was determined by the linear relationship:

$$\Delta G_D = \Delta G_D^{H_2O} - m[\text{GuHCl}] \quad (1)$$

where m is the slope of the line. For the calculation of ΔG_D, a two-state mechanism was assumed for the F (folded) → U (unfolded) transition. Hence, ΔG_D at a given guanidine concentration was determined using

$$\Delta G_D = -RT \ln\left(\frac{\theta_F - \theta}{\theta - \theta_U}\right) \quad (2)$$

where θ is the observed ellipticity at 220 nm and θ_F and θ_U are the ellipticities for the folded and unfolded states, respectively.

Renaturation Experiments. Lyophilized wild-type rIL-6 and the rIL-6 $Ala_{45,51,74,84}$ analog were dissolved in 6 M guanidine hydrochloride/0.1 M Tris-HCl, pH 8.6, and then equilibrated for 1 h at room temperature. Each protein solution was then diluted 10-fold, to a final concentration of 55 μg/mL, in stock solutions of guanidine hydrochloride ranging in concentration from 0 to 6 M and then equilibrated for 2 h before ellipticity measurements were performed at 220 nm, as previously described. After subtraction of the respective solvent backgrounds, data were expressed as percentages relative to the ellipticity measured in buffer alone, chosen as 100%.

Receptor Binding and Competitive Binding Inhibition Assays. Radioiodination of wild-type rIL-6 was performed as described by Bolton and Hunter (1974) and Taga et al. (1987). Bolton and Hunter reagent (2000 Ci/mmol) was purchased from Amersham. Radiolabeled rIL-6 was quantitated with a rIL-6-specific sandwich ELISA using the Genzyme "Interleukin-6 Interest Kit" (Inter Medico, Ontario, Canada). The rIL-6 was labeled to a specific activity of 7.8×10^7 cpm/μg. The affinity of wild-type rIL-6 for CESS cell IL-6 receptors was determined by Scatchard analysis of the direct binding data. Binding assays were performed essentially as described by Taga et al. (1987). Briefly, CESS cells obtained from ATCC were first cultured in RPMI 1640, 100 μg/mL streptomycin, 100 units/mL penicillin, 10% FCS, and 5% CO_2 at 37 °C. For the assay, cells were washed twice and incubated in RPMI 1640/25 mM Hepes, pH 7.2, supplemented with 3 mg/mL BSA, 100 μg/mL streptomycin, and 100 units/mL penicillin for 10 min at 37 °C. ^{125}I-rIL-6 was added to 10^6 cells in 0.1 mL of medium containing 0.1% NaN_3 in the presence or absence of a 200-fold excess of cold rIL-6 and incubated on ice with agitation for 4 h. After incubation, samples were layered onto a cushion of oil [1:1, v/v, bis(2-ethylhexyl) phthalate/dibutyl phthalate (Eastman Kodak Corp., Rochester, NY)] in 400-μL polypropylene tubes and centrifuged in a microfuge for 90 s at 9000 rpm. The tips of the tubes were cut and the cell pellets measured for radioactivity in a Beckman Model 8000 γ radiation counter. All assays were performed in triplicate.

For competitive binding inhibition assays, 100 μL of cell suspension (10^6 cells) was incubated with 0.66 ng of ^{125}I-rIL-6 and increasing concentrations of native rIL-6 or rIL-6 analogs at 4 °C for 4 h. Unbound ^{125}I-rIL-6 was removed by

centrifugation through oil as described above. The relative affinity of a rIL-6 variant for CESS cell IL-6 receptors was determined from the concentration giving 50% inhibition of ^{125}I-rIL-6 binding to CESS cells ($K_{I,app}$).

Epitope Mapping by Competitive Inhibition ELISAs. Mouse anti-human rIL-6 monoclonal antibodies 8 and 7 (mAb8 and mAb7) were generous gifts from Dr. L. Aarden (University of Amsterdam), and the mouse anti-human rIL-6 monoclonal antibody IG61 was kindly provided by Dr. N. Ida (N.I., Toray Industries). Inhibition ELISAs were performed as described by Brakenhoff et al. (1990). Briefly, microtiter plates were coated overnight at 4 °C with purified rIL-6 in PBS (with 2.0 μg/mL rIL-6 when using mAb8 and 1.0 μg/mL when using mAb7 or IG61). MAb7 (0.88 μg/mL), mAb8 (1.2 μg/mL), or IG61 (1.0 μg/mL) was preincubated in PBS, pH 7.4, 0.02% Tween 20, and 0.2% w/v gelatin (PGT) for 2 h at room temperature with serial dilutions of either wild-type rIL-6, mutant rIL-6, reduced and alkylated rIL-6 analogs, or rIL-6 denaturated by heat treatment for 40 min at 100 °C. After preincubation, antibody/rIL-6 complexes were transferred to rIL-6-coated microtiter plates and incubated for 2 h at room temperature. Plates were washed 3 times with PGT and then incubated 90 min with a 1:3000 dilution of a goat anti-mouse IgG (heavy and light chains) antibody (BRL) conjugated to alkaline phosphatase. Microtiter plates were developed using 0.5 mg/mL nitrophenyl phosphate as substrate in 10% v/v diethanolamine, 0.02% NaN_3, and 0.05 mM $MgCl_2$ and read at 405 nm in a Bio-Rad Model 450 microplate reader. All determinations were performed in duplicate in two independent experiments.

Bioassays. (A) BSF-2 (B-Cell Stimulatory Factor) Assay. BSF-2 assays were performed as described by Brakenhoff et al. (1989). Briefly, EBV-transformed SKW6.4 human B-cells (ATCC), which secrete a monoclonal IgM, were cultured in 24-well plates at a concentration of 5×10^3 cells/mL. Assays were carried out in 1 mL of MEM medium supplemented with 10% heat-inactivated FCS, 100 units/mL penicillin, 100 μg/mL streptomycin, and serial dilutions of the various rIL-6 species. After 4 days of incubation at 37 °C in 5% CO_2, the concentration of IgM secreted in culture supernatants was quantitated by an IgM-specific sandwich ELISA using a monospecific goat anti-human IgM antibody (BRL) for capture and the same antibody conjugated to horseradish peroxidase (HRP) (BRL) for detection. Plates were developed using 0.4 mg/mL *o*-phenylenediamine/H_2O_2 in 0.1 M citrate/phosphate, pH 4.5, as substrate. Color development was stopped with 4 M H_2SO_4, and microtiter plates were read at 492 nm. Assays were performed in duplicate using a purified human monoclonal IgM as standard. Comparisons between wild-type rIL-6 and analogs were made by determining the protein concentrations required to stimulate 50% maximal activity in three independent experiments.

(B) B9-Cell Proliferation Assay. The B-cell hybridoma proliferation assay was performed according to Helle et al. (1988) using the murine IL-6-dependent B13.29 (B9) cell line. The hybridoma was grown at 37 °C in MEM medium containing 5% FCS, supplemented with antibiotics, 1 nM human rIL-6, and 5% CO_2. Prior to the assay, cells were harvested by centrifugation and washed 3 times in IL-6-free medium. One thousand cells per well in 200 μL were cultured for 72 h at 37 °C in 96-well flat-bottom plates in the presence of increasing amounts of the various rIL-6 species. Cells were pulsed for 4 h with 2 μCi per well of [^{3}H]thymidine (Amersham, 185 GBq/mmol) and then harvested onto glass fiber filters and counted for radioactivity in a Searle Analytic Model 6892 liquid scintillation counter. Assays were performed in duplicate in three independent experiments. Comparisons between wild-type rIL-6 and analogs were made by determining concentrations required to stimulate 50% maximal [^{3}H]thymidine uptake.

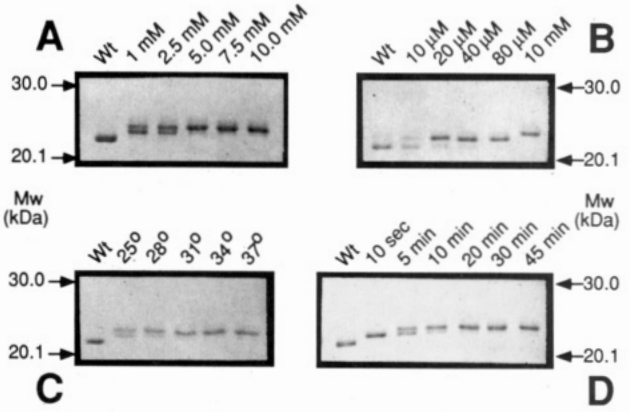

FIGURE 2: SDS–PAGE mobility shift analysis of reduced and alkylated rIL-6 species. Fifty microliter aliquots of rIL-6 (10 μM) in 0.1 M Tris-HCl, pH 8.6, were reduced under various conditions including DTT concentration (panels A and B), temperature (panel C), and time (panel D), as described under Materials and Methods. The values of the parameter tested in each individual experiment is indicated above the corresponding lane. SDS–polyacrylamide gels (15%) were prepared and electrophoresed as described by Laemmli et al. (1970) and visualized by staining with Coomassie blue.

Statistics. Statistical analyses were performed using the Wilcoxon's rank sum test.

RESULTS

Reduction and Alkylation Studies. The degree of solvent exposure of the two rIL-6 disulfide bonds was analyzed by testing their sensitivity to reduction using DTT. We previously demonstrated by SDS–PAGE analysis that fully reduced rIL-6 migrates slower than wild-type oxidized rIL-6 (Rock et al., 1992). Therefore, a mobility shift assay was used to determine the minimum molar ratio of DTT to rIL-6 required to fully reduce the molecule, under nondenaturing conditions.

Aliquots of rIL-6 were individually reduced for 1 h at 37 °C with DTT concentrations ranging from 0 to 10 mM and then alkylated and analyzed by SDS–PAGE (Figure 2A). Analysis of mobility shifts revealed that rIL-6 was fully reduced with a 500-fold molar excess of DTT (5 mM). However, at lower DTT concentrations, a rIL-6 species migrating between the native and fully reduced/alkylated forms was also detected (Figure 2B, lanes 2 and 3). We hypothesized that the fast-, intermediate-, and slow-migrating species corresponded to various S-carboxymethylated forms of rIL-6 representing native, partially (1-bridge) reduced, and fully reduced analogs, respectively. These findings suggested that one rIL-6 disulfide bond was substantially more labile to DTT reduction. To determine the amount of DTT required to completely convert native rIL-6 to this partially reduced form, we repeated the experiment using lower DTT concentrations (0–100 μM) (Figure 2B). Indeed, an intermediate species with one bridge reduced was generated with as little as a 4 molar excess of DTT over rIL-6 (40 μM DTT). The differential lability of the disulfide bridges was further examined in temperature-dependence and kinetic experiments. The effect of temperature on reduction was investigated by reducing rIL-6 with 5 mM DTT for 1 h at temperatures ranging from 25 to 37 °C. Samples were alkylated and immediately analyzed by SDS–PAGE for mobility shifts (Figure 2C). Both the single-bridge

and fully reduced forms were generated at 25 °C. However, the putative species with one bridge reduced could only be fully converted to the completely reduced form at temperatures greater than 34 °C. Kinetic experiments were conducted at 37 °C in the presence of 5 mM DTT (Figure 2D). Within 10 s after reduction initiation, rIL-6 was completely converted to the partially reduced form whereas complete reduction required at least 30-min incubation.

Identification of the Reduction-Labile Disulfide Bond. An HPLC peptide mapping approach was used to determine which bridge was most labile to reduction. One milliliter of a 10 μM solution of native rIL-6 was first partially reduced (1-bridge) with 4 molar excess DTT (40 μM) at 37 °C for 1 hour and then alkylated with iodo[2-^{3}H]acetic acid. To confirm that a partially reduced and radioalkylated form had been generated, a small aliquot of this preparation was first subjected to SDS–PAGE and autoradiography to confirm proper generation of the putative single-bridge reduced and alkylated species (Figure 3A, *inset*) and was subsequently digested with 4 μg of *S. aureus* V8 protease at 37 °C for 24 h.

V8 protease cleaves peptide bonds primarily at the C-terminus of glutamic acid residues. According to the published rIL-6 cDNA sequence (Hirano et al., 1986), complete digestion would theoretically generate 15 peptides, 3 of which should contain either 1 or 2 S-carboxymethylated cysteines: a 9-residue fragment (TCNKSNMCE), an 11-residue fragment (KDGCFQSGFNE), and a 12-residue peptide (TCLVKI-ITGLLE) containing both Cys_{45} and Cys_{51}, and Cys_{74} and Cys_{84}, respectively. However, disulfide linkage of the 2 latter peptides should result in a peptide fragment of 23 residues. The proteolytic fragments were separated by reverse-phase HPLC, and the radioactive fractions were collected. During the first round of HPLC purification, one minor peak with a retention time of 15.5 min was associated with greater than 80% of the radioactive counts (Figure 3A). To further resolve this peak, the radioactive fractions were pooled, lyophilized, and rechromatographed using a 0–20% acetonitrile gradient. The radioactive peak eluting with a retention time of 39.0 min (Figure 3B) was relyophilized, subjected to microsequence analysis, and shown to contain a single, nine-residue-long peptide (T[C]NKSNM[C]E), including two radioactive S-carboxymethylated residues (C) as judged by Microbore HPLC amino acid analysis using a PTH-S-carboxymethylated cysteine as standard. Moreover, the radioactive counts associated with each half-*S*-(carboxymethyl)cystine residue were found to be similar (14 350 cpm for Cys_{45} and 12 000 cpm for Cys_{51}), indicating little or no disulfide interchange. Thus, the reduction-labile disulfide bridge was detected as bridging Cys_{45} and Cys_{51}. Furthermore, the finding that only one radioactive peptide was isolated confirms that the rIL-6 band migrating between the native and fully reduced/alkylated species on SDS–PAGE is indeed a single-bridge, S-carboxymethylated rIL-6 variant.

Biophysical Analyses. A mutational strategy was chosen to determine the role of disulfide bond formation in rIL-6 folding and structural stabilization as well as to compare the structure–function relationships of reduced rIL-6 and rIL-6 cysteine mutants. Three disulfide bond-deficient rIL-6 analogs were constructed in which either a pair of cysteines (Cys_{45}/Cys_{5}31 or Cys_{74}/Cys_{84}) or all four cysteines were replaced with alanines. Cysteine residues were substituted with Ala instead of Ser because Ala not only is tolerated in a wide variety of secondary structures but also best approximates the hydrophobic nature of the native, oxidized cysteines.

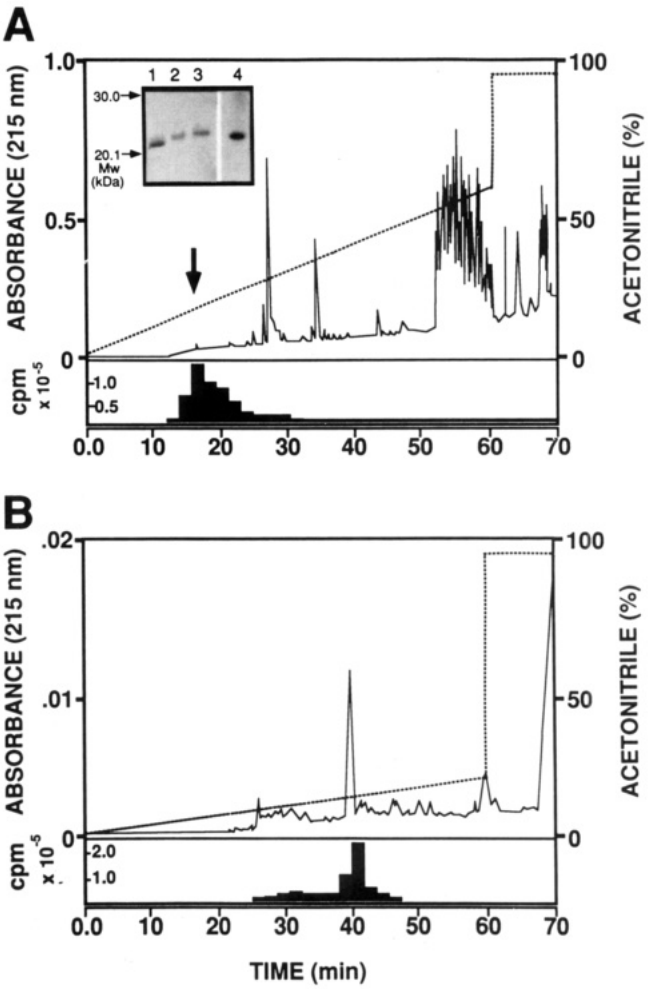

FIGURE 3: Reverse-phase HPLC peptide mapping. (Panel A, inset) SDS–PAGE analysis of wild-type and reduced rIL-6 species. Wild-type rIL-6 was reduced with a 4-fold molar excess of DTT and then labeled with iodo[2-^{3}H]acetic acid. Radioactive incorporation was verified by autoradiography of an SDS–polyacrylamide gel (15%). Lane 1, wild-type rIL-6; lane 2, rIL-6 reduced with a 4-fold molar excess of DTT at 37 °C for 1 h, lane 3, rIL-6 reduced with 10 mM DTT at 37 °C for 1 h; lane 4, autoradiograph of sample shown in lane 2. The radiolabeled sample was digested with *S. aureus* V8 protease at 37 °C for 24 h, and 200 μg was applied to an analytical Vydac C_{18} column (0.46 × 25 cm). Peptides were eluted using a 0–60% acetonitrile gradient in 0.1% TFA developed over 60 min at a flow rate of 0.8 mL/min. Peptide elution was monitored by UV absorbance at 215 nm and liquid scintillation counting (lower panel). One radioactive peak (arrow) was collected, lyophilized, and rechromatographed. (Panel B) Peptides were rechromatographed using a 0–20% acetonitrile gradient in 0.1% TFA developed over 60 min at a flow rate of 0.8 mL/min. The radioactive peak was collected manually and subjected to microsequencing for identification.

Analogs are designated rIL-6 $Ala_{45,51}$, rIL-6 $Ala_{74,84}$, and rIL-6 $Ala_{45,51,74,84}$, respectively.

Circular Dichroism Studies. Small differences in SDS–PAGE mobilities of the purified rIL-6 Ala mutants and wild-type rIL-6 were observed (data not shown), suggesting possible conformational differences. To further investigate these differences, far-UV CD analyses were performed to compare the α-helical contents of rIL-6 alanine analogs with those of wild-type rIL-6 as well as reduced/alkylated rIL-6 species. All far-UV CD spectra (Figure 4) exhibited ellipticity minima at 208 and 222 nm characteristic of an α-helical structure. The α-helical content of rIL-6 $Ala_{45,51}$ was found to be identical to that of wild-type rIL-6 with $f_{helix} = 0.70$, $f_{sheet} = 0.25$, and $f_{remaining} = 0.05$. However, both the $Ala_{74,84}$ and $Ala_{45,51,74,84}$ rIL-6 mutants displayed a 16% reduction in α-helicity.

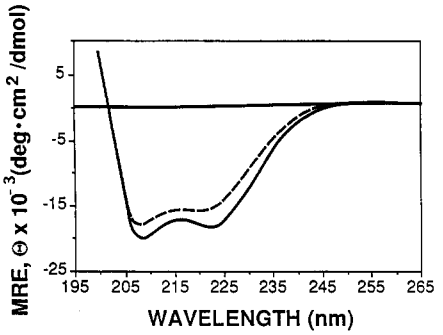

FIGURE 4: Circular dichroism analysis. Experimental far-UV CD spectra obtained for HPLC-purified wild-type rIL-6 and rIL-6 $Ala_{45,51}$ (—) and rIL-6 $Ala_{74,84}$ and rIL-6 $Ala_{45,51,74,84}$ (- - -) molecules. Protein concentrations were determined by UV absorbance using an extinction coefficient ($E^{1\%}_{1cm}$) of 4.6 at 280 nm (Rock et al., 1992). Measurements were performed between 200 and 260 nm as described under Materials and Methods. Spectra represent the averages of three independent determinations. The standard deviation was found to be ±4% MRE at 220 nm.

Interestingly, the far-UV spectra of the single-bridge and fully reduced/alkylated species were indistinguishable from that of wild-type rIL-6 (data not shown).

Denaturation and Refolding Studies. To test whether the second disulfide bridge of IL-6 stabilizes its secondary structure, wild-type rIL-6, fully reduced but not alkylated rIL-6, and the rIL-6 cysteine-less mutant were denatured in the presence of increasing concentrations of guanidine hydrochloride. Changes in α-helicity were monitored at 220 nm. Denaturation curves were virtually superimposable, with a transition point at 3.7 M GuHCl (Figure 5A), indicating that all rIL-6 species exhibited the same degree of secondary structure stability. Indeed, the change in free energy observed for GuHCl-induced α-helix unfolding was calculated to be −19.2 kJ/mol, a value similar to that obtained with hG-CSF (Lu et al., 1992).

The wild-type rIL-6 molecule could be reversibly refolded from a fully denatured conformation to its native state. In contrast, the cysteine-less mutant regained only 80% of wild-type α-helicity (Figure 5B), suggesting the coexistence of folded and unfolded species.

Immunochemical Analysis. Changes in tertiary structure were monitored by competitive inhibition ELISAs using a panel of three anti-IL-6 monoclonal antibodies. MAb8 is a neutralizing antibody recognizing a conformation epitope involving residues from both the N- and C-terminal ends of the molecule (Brakenhoff et al., 1990). Reduced/alkylated rIL-6 lacking the first disulfide bridge and the rIL-6 $Ala_{45,51}$ variant were equally potent at inhibiting antibody binding to solid-phase rIL-6 (Figure 6A,B). In contrast, fully reduced/alkylated rIL-6 and both the rIL-6 $Ala_{74,84}$ and rIL-6 $Ala_{45,51,74,84}$ mutants were unable to significantly compete for mAb8 binding even at concentrations up to 15 μg/mL. The neutralizing antibody IG61, which recognizes an epitope (residues Ala_{154}–Thr_{163}) located at the N-terminus of the D helix (Ida et al., 1989), reacted equally well with all rIL-6 species tested (data not shown), indicating that this epitope is exposed and does not require disulfide bond formation for expression. Surprisingly, the IG61 mAb exhibited a low affinity for heat-denatured rIL-6, probably as a result of a decrease in surface accessibility caused by conformational perturbations. In contrast to the previous antibodies, mAb7 recognizes a hidden epitope (cryptotope) within the putative IL-6 CD loop (residues Thr_{143}–Ala_{146})) and exhibits a higher affinity for denatured rIL-6 than for wild-type rIL-6 (Brakenhoff et al., 1990). Interestingly, of all rIL-6 analogs tested,

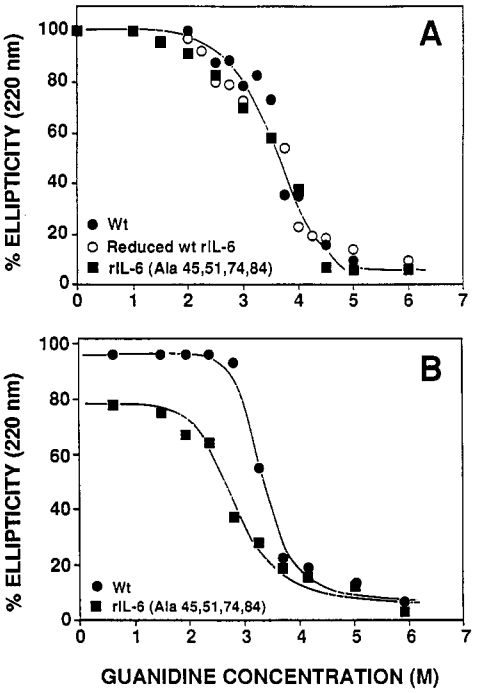

FIGURE 5: Denaturation and refolding of native rIL-6 and rIL-6 analogs. For denaturation studies (panel A), rIL-6 species (final concentration between 75 and 100 μg/mL) were 20-fold diluted with increasing concentrations of guanidine hydrochloride in 0.1 M Tris-HCl, pH 8.6. In one experiment, wild-type rIL-6 was fully reduced with 10 mM DTT and subsequently denatured in guanidine solutions containing 2 mM DTT to prevent reoxidation. For refolding (panel B), rIL-6 species were first dissolved in 6 M guanidine hydrochloride/0.1 M Tris-HCl, pH 8.6, and then diluted 10-fold to a concentration of 55 μg/mL with 0–6 M guanidine solutions. After equilibration, ellipticities were measured at 220 nm and 25 °C. After subtraction of the respective solvent spectra, ellipticities were calculated and expressed as percentages relative to the MRE obtained in the buffer alone, taken as 100%. Each data point represents the mean of four determinations.

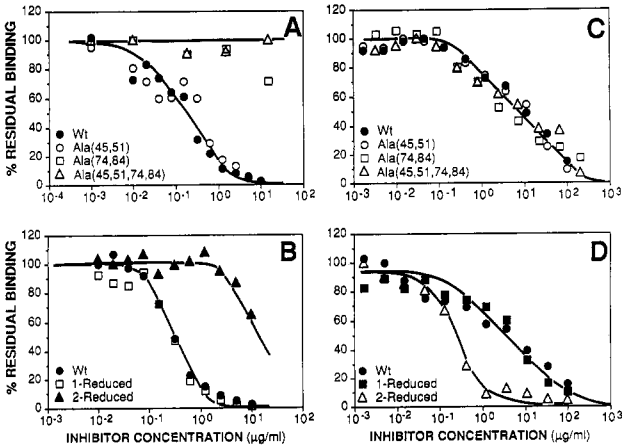

FIGURE 6: Competitive inhibition ELISAs. Inhibition of mAb8 (panels A and B) and mAb7 (panels C and D) binding to solid-phase wild-type rIL-6 by various rIL-6 analogs was analyzed as described under Materials and Methods. MAb8 (1.2 μg/mL) or mAb7 (0.88 μg/mL) was preincubated with increasing amounts of rIL-6 analogs for 2 h at 25 °C after which the percent residual binding was determined by ELISA. The graph depicted is representative of one typical experiment. Each point represents the mean of duplicate determinations.

only the fully reduced/alkylated rIL-6 molecule reacted with mAb7 with enhanced affinity (Figure 6C,D), suggesting a significantly altered tertiary conformation.

Functional Activity of Wild-Type rIL-6 and rIL-6 Analogs. To determine whether structural alterations correlated with

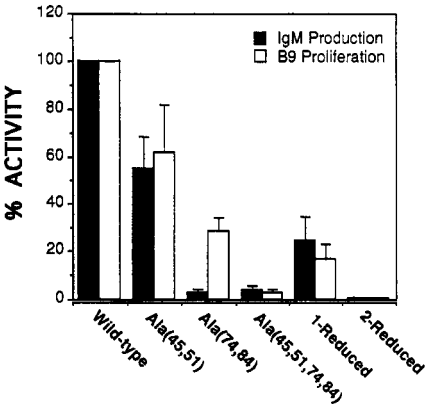

FIGURE 7: Biological activities of rIL-6 analogs. Wild-type rIL-6, reduced and alkylated rIL-6 species, and rIL-6 cysteine mutants were assessed for their ability to stimulate IgM production in SKW6.4 cells and the growth of B9 cells as described under Materials and Methods. The relative functional activity of each rIL-6 species was determined as the concentration required for 50% maximal activity. Values are expressed as percentages relative to those obtained with wild-type rIL-6 chosen as 100%. Each bar represents the mean of three independent determinations performed in triplicate.

changes in biological activity, the various rIL-6 species were tested in both the B9 proliferation and SKW6.4 differentiation assays. Results from these experiments are summarized in Figure 7. The rIL-6 $Ala_{45,51}$ mutant exhibited a minor 41% decrease in activity whereas the reduced/alkylated rIL-6 species lacking the first disulfide bridge displayed approximately 75% reduction in both assays. In contrast, the functional activities of rIL-6 species lacking both disulfide bridges were markedly impaired in both bioassays as illustrated by a residual, 3.7% and 0.5%, wild-type activity for the cysteine-less mutant and the fully reduced/alkylated rIL-6 analog, respectively. Interestingly, the rIL-6 $Ala_{74,84}$ mutant exhibited markedly different responses depending on the assays since it retained 28% and 2.7% wild-type activity in the B9 proliferation and BSF-2 assay, respectively.

To determine if the observed reduction in activity of the reduced/alkylated rIL-6 analogs was due either to the negative charge of iodoacetic acid and/or to the steric hindrance of the bulky carboxymethyl group, we comparatively tested rIL-6 molecules alkylated with either iodoacetic acid ($IAcO^-$), iodoacetamide ($IAcNH_2$), or methyl iodide (CH_3I). Iodoacetamide and methyl iodide alkylate cysteine residues with an uncharged methyl amine group and a smaller methyl group, respectively. The observed deficiencies in the ability of reduced/alkylated analogs to stimulate B9 cell profileration were found to be independent of the alkylating agent (data not shown).

Receptor Binding Assays. The IL-6 receptor is an $\alpha\beta$ heterodimer, transmembrane signaling is initiated by the interaction of IL-6 with an 80-kDa glycoprotein, the receptor α-chain. This complex then interacts with the nonligand binding, 130-kDa glycoprotein (β-chain), which mediates signal transduction (Taga et al., 1989). The coupling of the α- and β-chains of the IL-6 receptor (IL-6R) is required for high-affinity IL-6/IL-6R interaction (Taga et al., 1989). Scatchard analysis of direct binding data indicated that the K_d of IL-6 for CESS cell receptors was 0.31 nM (data not shown), similar to the value previously reported by Taga et al. (1987). The relative affinities of CESS cell IL-6R for rIL-6 analogs were assessed in competitive binding inhibition assays (Figure 8A,B). The $K_{I,app}$ values for rIL-6 cysteine mutants and S-carboxymethylated rIL-6 species are summarized in Table 1. The receptor binding activities of

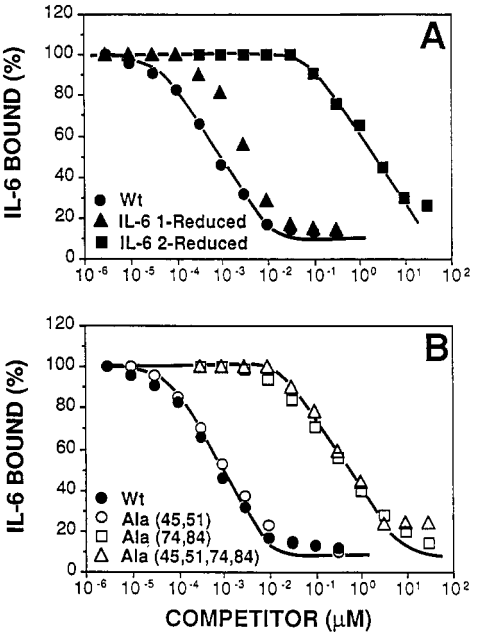

FIGURE 8: Competitive receptor binding inhibition assays. The affinities of IL-6 variants for CESS (10^6 cells) receptors were assessed by their ability to compete with wild-type ^{125}I-rIL-6 molecules. Varying concentrations of rIL-6 analogs were mixed with the amount of ^{125}I-rIL-6 required to saturate 50% of receptor sites. After subtraction of nonspecific binding, data were plotted as percent radioligand bound vs the log of IL-6 competitor concentration. Each point represents the mean of three independent determinations. 100% binding was defined as the amount of ^{125}I-rIL-6 bound to CESS cells in the absence of competitor.

Table 1: Apparent Affinities of rIL-6 Analogs

analog[a]	$K_{I,app}$ (nM)[b]
Wt	1.0
$Ala_{45,51}$	1.5
$Ala_{74,84}$	350
$Ala_{45,51,74,84}$	400
1-reduced	3.0
2-reduced	2000

[a] rIL-6 analogs. Mutant proteins were created by Cys to Ala substitutions at amino acid positions designated by subscripts. [b] Determined by competitive inhibition assay and calculated as described under Materials and Methods.

molecules lacking the first disulfide bridge were comparable to that of wild-type rIL-6, whereas those of the three analogs lacking the second disulfide bridge were markedly reduced (1/350 to 1/2000). The decrease in functional activity observed for fully reduced/alkylated rIL-6, rIL-6 $Ala_{74,84}$, and rIL-6 $Ala_{45,51,74,84}$ did not correlate with the reduction in their respective $K_{I,app}$ values. For example, the cysteine-less mutant only exhibited 3.7% wild-type activity in two bioassays in spite of a 0.25% residual receptor binding activity. This may be explained by the fact that high-affinity receptor binding may not be required for signal transduction (Shanafelt & Kastelein, 1993) or that partial receptor occupancy is sufficient for mediating full biological activity, or both.

DISCUSSION

Previous site-directed mutagenesis experiments revealed that the disulfide bridge formed between Cys_{74} and Cys_{84} is essential for full biological activity and receptor binding (Snouwaert et al., 1991a). However, it is not possible to assess from these studies whether the functional defects observed are due to gross perturbations resulting from incorrect folding of cysteine-deficient rIL-6 analogs or to local conformational changes

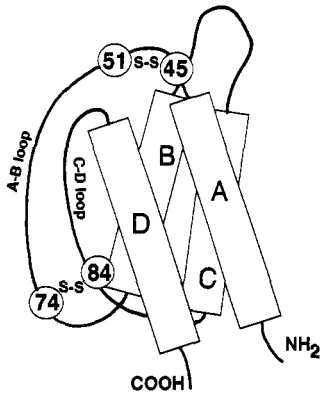

FIGURE 9: Schematic representation of the putative rIL-6 four α-helix bundle structure. The model is adapted from Bazan (1990) and Hill et al. (1993). The four antiparallel helices are represented by rectangular boxes and are labeled A–D. Circled numbers indicate the positions of cysteine residues, the "S–S" represent the covalent disulfide bonds.

affecting the receptor binding site(s). To address this question, we have reanalyzed the respective structural and functional importance of the two disulfide bridges by comparing the secondary structure, the antigenicity, the receptor binding activity, and the biological properties of reduced/alkylated rIL-6 species as well as three rIL-6 cysteine mutants.

To this end, two different types of disulfide bond-deficient rIL-6 analogs were generated. The first set of rIL-6 analogs was produced by selective chemical cleavage of disulfide bonds to provide insights into the role of cystines in the maintenance of the cytokine's structure, stability, and function. A second panel of IL-6 variants was engineered by site-directed mutagenesis whereby naturally bonded cysteines were replaced in pairs by alanines. These rIL-6 mutants were used not only to corroborate the results obtained with the chemically reduced/alkylated analogs but also to assess the role played by each disulfide bridge in the correct refolding of denatured rIL-6.

Assuming by analogy with hGRH (Bazan, 1990; DeVos et al., 1992) and hG-CSF (Hill et al., 1993) that IL-6 contains four antiparallel α-helices (A–D) connected by flexible loops (Figure 9), the first Cys_{45}–Cys_{51} bridge would clip the N-terminal end of the AB loop whereas the second Cys_{74}–Cys_{84} bond would fasten the C-terminal end of the AB loop to the B helix. These two disulfide bonds were shown to exhibit markedly different sensitivities to reduction. Selective and complete reduction of the first disulfide bridge (Cys_{45}–Cys_{51}) was achieved with 100-fold less molar amounts of DTT, at lower temperature, and at a faster rate than the second bridge. These findings suggest that the two disulfide bridges reside in different surface microenvironments and that the first bridge is more exposed to solvent or, alternatively, may have a higher reduction potential.

Both the partially reduced/alkylated rIL-6 (1-bridge) and the rIL-6 ($Ala_{45,51}$) mutant lacking the first disulfide bond exhibited structural properties similar to those of native rIL-6, as judged by their similar α-helix content. The antigenicity of both molecules probed with three different anti-IL-6 monoclonal antibodies, mAb7, mAb8, and IG61, was indistinguishable from that of wild-type rIL-6. The rIL-6 $Ala_{45,51}$ mutant was found to be as potent as native rIL-6 in the receptor binding assay although it was consistently less active in the BSF-2 and B9 proliferation assays. In spite of its apparent structural integrity, the partially reduced/alkylated rIL-6 analog exhibited a 66% and 75% decrease in receptor binding and functional activity, respectively. These results provide evidence that the region surrounding the Cys_{45}–Cys_{51} bond may be involved in IL-6/IL-6R interaction and/or signal transduction and support the previous hypothesis by Snouwaert et al. (1991a) that this bond plays a role in maintaining full rIL-6 biological activity.

In contrast, the structural and biological properties of fully reduced/alkylated rIL-6, rIL-6 $Ala_{74,84}$, and the cysteine-less analog were drastically altered. Although previous studies clearly demonstrated that functional importance of the second disulfide bridge (Snouwaert et al., 1991a; Jean et al., 1993), no structural correlations were established. Indeed, we found that molecules lacking this bridge were partially unfolded as demonstrated by their markedly decreased reactivity with mAb8. However, the fully reduced/alkylated rIL-6 molecule was shown to be more denatured than either the rIL-6 $Ala_{74,84}$ mutant or the cysteine-less analog, since it was the only species to react with mAb7 with enhanced affinity. Interestingly, in all three species, the D-helix epitope recognized by IG61 was unaltered, suggesting that these molecules still retain some nativelike conformation. The structural changes affecting the conformational mAb8 epitope related to the IL-6 active site were correlated with a decrease in CESS cell receptor binding activity between 0.05% and 0.29%. However, differences were observed in the residual biological activities of these three rIL-6 species. The BSF-2 activity of the two cysteine mutants was reduced to 3.3%. A similar decrease was observed with the cysteine-less mutant in the murine B9-cell proliferation assay whereas the mutant lacking only the second disulfide bridge retained 30% of wild-type activity. This observation confirms the previous findings by Snouwaert et al. (1991b) that rIL-6 cysteine mutants are significantly more active in rodent cells than in human cells. Surprisingly, the fully reduced and S-carboxymethylated rIL-6 was found to be 1 order of magnitude less active than the two cysteine analogs regardless of the cell types used in the bioassays. This finding suggests that the residual activity of fully reduced/alkylated rIL-6 is unlikely due to a contamination with trace amounts of partially reduced and/or unreduced molecules. Nevertheless, whether alkylation *per se* contributes to this drastic reduction in activity remains to be demonstrated. However, the impairment in receptor binding and functional activities of these three rIL-6 species seems to be essentially due to local conformational changes since their α-helix contents were comparable. The Cys_{74}–Cys_{84} disulfide bridge appears to be indispensable for maintaining the structural integrity of the primary IL-6 receptor binding site. If this bridge directly links the AB loop with the B helix, it may be necessary to maintain a loop–helix interaction known to play a significant stabilizing role in proteins with four-helix bundles (Chou et al., 1992). Full reduction might destabilize the relative orientation of the A and D helices, accounting for the loss in mAb8 epitope antigenicity. Alternatively, reduction of the second bridge alone could affect the tertiary structure of the AB loop which, by analogy with hGRH, might also contribute to the formation of the receptor binding site.

Protein folding pathways are thought to encounter activation barriers and therefore produce specific folding intermediates (Kim & Baldwin, 1990). The formation of a disulfide bond between Cys residues 74 and 84 may serve as an "adhesion step" which locks the AB loop and B helix into an intermediate subdomain conformation preceding the folding of the receptor binding site. The absence of enhanced reactivity of mutants lacking the second disulfide bridge with mAb7, their wild-type-like reactivity with mAb IG61, and their substantial residual biological activity clearly indicate that they are not

grossly misfolded. However, the lack of formation of this bridge did not allow proper folding of the active site as demonstrated by the reduced mAb reactivity. Furthermore, in contrast to wild-type rIL-6, renaturation experiments suggested that refolding of the cysteine-less mutant yielded a mixed population of folded and unfolded conformers. Nonetheless, the second bridge does not seem to play a critical role in stabilizing rIL-6 α-helical structure since the denaturation curves for all rIL-6 species were virtually indistinguishable.

IL-6 and hG-CSF share 26% sequence similarity and conserved disulfide bond patterns. However, the hG-CSF and IL-6 disulfide bonds have different conformational roles since, in hG-CSF, they are required to maintain the integrity of both the secondary and tertiary structures of the cytokine (Kuga et al., 1989; Layton et al., 1991; Lu et al., 1992).

In conclusion, we have shown that the first disulfide bridge of IL-6 is highly labile and plays a minor functional role but yet is required for full biological activity. In contrast, the second bridge is more resistant to reducing agents and is critical in both directing the proper folding of the molecule and maintaining the structural integrity and antigenicity of its primary receptor binding site.

ACKNOWLEDGMENT

We thank Dr. Lucien Aarden for the generous gift of the mAb8 and mAb7 monoclonal antibodies and Dr. Robert Painter for the use of the Gilson HPLC apparatus. We also thank Dr. David Isenman for insightful discussions throughout the course of this study.

REFERENCES

Abdel-Meguid, S. S., Sheih, H. S., Smith, W. W., Dayringer, H. E., Violand, B. N., & Bentle, L. A. (1987) *Proc. Natl. Acad. Sci. U.S.A. 84*, 6434–6437.

Bazan, J. F. (1990) *Immunol. Today 11*, 350–354.

Bolton, A. E., & Hunter, W. M. (1974) *Biochem. J. 133*, 529–538.

Brakenhoff, J. P., Hart, M., & Aarden, L. A. (1989) *J. Immunol. 143*, 1175–1182.

Brakenhoff, J. P., Hart, M., DeGroot, E. R., Di Padova, F., & Aarden, L. A. (1990) *J. Immunol. 145*, 561–568.

Chou, K. C., Maggiora, G. M., & Scheraga, H. A. (1992) *Proc. Natl. Acad. Sci. U.S.A. 89*, 7415–7419.

Clogston, C. I., Boone, T. C., Crandall, C., Mendiaz, E. A., & Lu, H. S. (1989) *Arch. Biochem. Biophys. 272*, 144–151.

De Vos, A. M., Ultsch, M., & Kossiakoff, A. A. (1992) *Science 255*, 306–312.

Fiorillo, M. T., Cabibbo, A., Iacopetti, P., Fattori, E., & Ciliberto, G. (1992) *Eur. J. Immunol. 22*, 2609–2615.

Helle, M., Boeije, L., & Aarden, L. A. (1988) *Eur. J. Immunol. 18*, 1535–1540.

Hill, C. P., Osslund, T. D., & Eisenberg, D. (1993) *Proc. Natl. Acad. Sci. U.S.A. 90*, 5167–5171.

Hirano, T., Yasukawa, K., Harada, H., Taga, T., Watanabe, Y., Matsuda, T., Kashiwamura, S., Nakajima, K., Koyama, K., Iwamatsu, A., Tsunasawa, S., Sakiyama, F., Matsui, H., Takahatra, Y., Taniguchi, T., & Kishimoto, T. (1986) *Nature 324*, 74–76.

Hirano, T., Akira, S., Taga, T., & Kishimoto, T. (1990) *Immunol. Today 11*, 443–449.

Ida, N., Sakurai, Touko, H., Hosoi, K., Kunitomo, T., Shimazu, T., Maruyana, T., Matsuura, Y., & Kohase, M. (1989) *Biochem. Biophys. Res. Commun. 165*, 728–734.

Jambou, R. C., Snouwaert, J. N., Bishop, G. A., Stebbins, J. R., Frelinger, J. A., & Fowlkes, D. A. (1988) *Proc. Natl. Acad. Sci. U.S.A. 85*, 9426–9430.

Jean, L. L., Waters, C. A., Keemy, D., & Murphy, J. R. (1993) *Protein Eng. 6*, 305–311.

Kim, P. S., & Baldwin, R. L. (1990) *Annu. Rev. Biochem. 59*, 631–660.

Krüttgen, A., Rose-John, S., Möller, C., Wroblowski, B., Wollmer, A., Müllberg, J., Hirano, T., Kishimoto, T., & Heinrich, P. C. (1990) *FEBS Lett. 262*, 323–326.

Kuga, T., Komatsu, Y., Yamasaki, M., Okabe, M., Morimoto, M., & Itoh, S. (1989) *Biochem. Biophys. Res. Commun. 159*, 103–111.

Laemmli, U. K., Molbert, E., Showe, M., & Kellenberger, E. (1970) *J. Mol. Biol. 49*, 99–113.

Layton, J. E., Morstyn, G., Fabri, L. J., Reid, G. E., Burgess, A. W., Simpson, J. R., & Nice, E. C. (1991) *J. Biol. Chem. 266*, 23815–23823.

Leutz, A., Damm, K., Sterneck, E., Kowenz, E., Ness, S., Frank, R., Gausepohl, H., Pan, Y., Smart, J., Hayman, M., & Graf, T. (1989) *EMBO J. 8*, 175–181.

Lu, H. S., Boone, T. C., Souza, L. M., & Lai, P. H. (1989) *Arch. Biochem. Biophys. 268*, 81–92.

Lu, H. S., Clogston, C. L., Narhi, O. L., Merewether, L. A., Pearl, W. R., & Boone, T. C. (1992) *J. Biol. Chem. 267*, 8770–8777.

Provencher, S. W., & Glöckner, J. (1981) *Biochemistry 20*, 33–37.

Rock, F., Everett, M., & Klein, M. (1992) *Protein Eng. 5*, 583–591.

Sambrook, J., Fritsch, E. F., & Maniatis, T. (1989) in *Molecular Cloning: A Laboratory Manual* (Ford, N., Ed.) 2nd ed., Vol. 2, Cold Spring Harbor Laboratory Press, Cold Spring Harbor, NY.

Shanafelt, A. B., & Kastelein, R. A. (1992) *J. Biol. Chem. 267*, 25466–25472.

Simpson, R. J., Moritz, R. L., Van Roost, E., & Van Snick, J. (1989) *Biochem. Biophys. Res. Commun. 157*, 364–372.

Snouwaert, J. N., Leebeek, F. W. G., & Fowlkes, D. M. (1991a) *J. Biol. Chem. 264*, 23097–23102.

Snouwaert, J. N., Kariya, K., & Fowlkes, D. M. (1991b) *J. Immunol. 146*, 585–591.

Taga, T., Kawanishi, Y., Hardy, R., Hirano, T., & Kishimoto, T. (1987) *J. Exp. Med. 166*, 967–981.

Taga, T., Hibi, M., Hirata, Y., Yamasaki, K., Yasukawa, K., Matsuda, T., Hirano, T., & Kishimoto, T. (1989) *Cell 58*, 574–581.

Tanabe, O., Akira, S., Kamiya, T., Wong, G. G., Hirano, T., & Kishomoto, T. (1988) *J. Immunol. 141*, 3875–3881.

Tsuchiya, M., Asano, S., Kaziro, Y., & Nagata, S. (1986) *Proc. Natl. Acad. Sci. U.S.A. 84*, 7633–7637.

Van Snick, J. (1990) *Annu. Rev. Immunol. 8*, 253–278.